Spatial-Spectral Classification of Hyperspectral Images Based on Extended Morphological Profiles and Guided Filter

Research Article

Behnam Asghari Beirami*[1]   Mehdi Mokhtarzade [2]

Abstract. Previous studies show that the incorporation of spatial features in the classification process of hyperspectral images (HSI) improves classification accuracy. Although different spatial-spectral methods are proposed in the literature for the classification of the HSI, they almost have a slow, complex, and parameter-dependent structure. This paper proposes, a simple, fast and efficient two-stage spatial-spectral method for the classification of the HSI based on extended morphological profiles (EMP) and the guided filter. The proposed method consists of four major stages. In the first stage, principal component analysis (PCA) is used to smooth the HSI to extract the low-dimensional informative features. In the second stage, EMP is produced from the first three PCs. Stacked feature vectors, consisting of PCs and EMP, are classified via support vector machines (SVM) in the third step. Finally, a post-processing stage based on a guided filter is applied to classified maps to further improve the classification accuracy and to refine the noisy classified pixels. Experimental results on two famous hyperspectral images named Indian Pines and Pavia University in a very small training sample size situation show that the proposed method can reach the high level of accuracies which are superior to some recent state-of-the-art methods.

Keywords. Extended Morphological Profiles, Guided Filter, Support Vector Machine, Principal Components Analysis, Hyperspectral, Classification.

1. Introduction

Hyperspectral images (HSI) contain rich spectral information that can be used in various fields of earth science studies such as identifying the different material, geology, forest, and investigating the changes of earth surface land-covers. Due to the high dimensionality of the HSI (large numbers of spectral bands) and the limited size of the training samples, supervised classification of the HSI is challenging and commonly leads to curse of dimensionality [1]. Besides, inter-class spectral variability and intra-class spectral similarity may deteriorate the classification accuracy.

Based on the literature, different methods are proposed to address the curse of dimensionality in the classification of the HSI. Generally, they are grounded in three major groups:

- Dimensionality reduction (DR) techniques: Different feature extraction and feature selection methods are proposed in the literature to efficiently reduce the dimension of the HSI. Principal component analysis (PCA) [2], independent component analysis (ICA) [2], kernel principal component analysis (KPCA) [3], Fisher's linear discriminant analysis (FLDA) [4], locality adaptive discriminant analysis (LADA) [5], ensemble discriminative local metric learning (EDLML) [6], minimum noise fraction (MNF) [2], and mutual information band selection [7] are among the most important classical approaches. Developing the new efficient DR methods are still a hot topic, and in recent years different novel methods such as SuperPCA [8], band grouping SuperPCA [9], and kernel SuperPCA [10] are proposed for HSI feature extraction.

- Advanced classifiers: Different advanced classifiers that are less sensitive to the size of training samples such as support vector machines (SVM) [11], extreme learning machines (ELM) [12], sparse representation classifier (SRC) [13], collaborate representation classifier (CRC) [13], and random multi-graphs (RMG) [14] are used in the literature for classification of the HSI.

- Generating the virtual training samples: Numerous data augmentation, and virtual training samples generation methods such as Generative adversarial network (GAN) [15], and Gaussian mixture model (GMM) [16] are proposed in the literature for efficient classification of the HSI.

- To address the second issue about the inter-class spectral variability and intra-class spectral similarity, numerous studies have proved the efficiency of incorporating textural and spatial features in traditional spectral based classification [11]. The main idea of using the spatial features in the classification of the HSI is supported by this concept that the near pixels are usually grounded in the same class.

Morphological profiles (MP) are one of the most promising spatial features for the classification of the HSI. Morphological opening and closing that are based on elementary dilation and erosion operators are used to extract bright/dark features [17]. Morphological profiles are produced by geodesic opening and closing operators [18]. The extended morphological profiles (EMP) are the adoption of the MP to multi-band images [17]. In this method, because of the high dimensionality of the HSI, MP is produced from the first few PCs. A method based on MP and multi-kernel SVM is proposed in [19]. Their final results show that classifying morphological and spectral feature with multi-kernel SVM reached to higher accuracies. The

[1]* B. Asghari Beirami, Ph. D student, Department of photogrammetry and remote sensing, K. N. Toosi University of Technology, Tehran, Iran. Email: b_asghari@email.kntu.ac.ir

[2] M. Mokhtarzade, Associate professor, Department of photogrammetry and remote sensing, K. N. Toosi University of Technology, Tehran, Iran. Email: m_mokhtrzade@kntu.ac.ir

accuracy of the EMP-based classification is greatly influenced by the types of the structuring element (SE). In [20], multiple classifier systems based on EMP are proposed in which EMPs with multi-shapes SEs are used to better detect the structures in the image. The EMPs created from SEs of different shapes are independently classified, and the final classification map is produced by decision fusion.

In addition to using spatial features such as EMP in the pre-processing stage, spatial information can be used in the post-processing phase to improve the classification accuracy of the HSI. The guided filter (GF) is an edge-preserving filter which is faster than other edge-preserving filters such as anisotropic diffusion or bilateral filter and has good behavior near the edges and does not cause a false edge [21]. In recent years, this filter is used in some studies in the field of hyperspectral image processing. A novel method is introduced in [22] that combines PCs, GF and the random forest classifier. In this method, after dimensionality reduction by PCA, the edge-preserving GF is used to smooth the HSI and to extract the spatial features. In [23] GF is used in the post-processing stage of hyperspectral image classification to smooth the results of SVM classification. In [24], an ensemble classification technique based on the weighted ensemble of hierarchical GF and matrix of spectral angle distance are proposed for classification of the HSI. A good comparative study was carried out in [25] for investigating the impact of different filtering methods in pre and post-processing stages on the accuracy of the HSI classification.

Although the EMP and guided filter are used individually in the mentioned studies, there is still some issue that should be addressed. 1) Although the previous methods based on EMP [17,18] and GF [23] individually are fast and efficient, they may not reach a high level of accuracy, especially when the limited training samples are available. 2) Some of the previous proposed spatial-spectral methods are complex such as [26] or have the time-consuming performance such as deep models [27, 28]. To address previously mentioned issues, this paper proposes a simple, fast and accurate two-stage HSI spatial-spectral classification method (named EMP-GF). The main contributions of the EMP-GF are as follows:

1) For the first time in literature, in this study, EMP-GF integrates the PCA feature extraction, SVM classifier without the cross-validation, extended morphological profiles (EMP), and a post-processing stage based on the guided filter.

2) EMP-GF has great performance even when the very limited training samples are available. Also, EMP-GF is superior over some recent state-of-the-art methods.

We validate the proposed method in the classification of two challenging hyperspectral images from agricultural and urban areas.

Section 2 proposes the methodology of the EMP-GF. Section 3 presents the data set and the experimental results. At last, conclusions are summarized in Section 4.

2. Methodology

Based on Fig. 1 that shows the block diagram of proposed EMP-GF, this method consists of six major steps as follows:
1) In the first step, to eliminate the noise and to improve the performance of PCA, HSI is smoothed with the simple mean filter. In this method, a sliding window with the size 3×3 is considered around each pixel in each band of the HSI and the mean of the gray level values of the image in this window is considered as the final value of each pixel in each band.

2) In the second step, to overcome the course of dimensionality, PCA is used for feature extraction of the HSI.

3) In the third step, to address the issue of inter-class spectral variability and intra-class spectral similarity, spatial features based on EMP are produced from the first three principal components analysis (PCs). Later, EMP stacked to the spectral feature vectors that consist of PCs and form the spatial-spectral feature vectors.

4) Resultant spatial-spectral feature vectors are classified with SVM without using the cross-validation due to its huge processing time. A normalization technique and polynomial kernel based on [29] are used for fast and efficient training of SVM.

5) To further the classification accuracy, as the post-processing stage, the guided filter is applied based on gray and color guidance images on initial probability maps that are obtained from SVM.

6) In the last step, the label of each pixel is determined based on the maximum probability rule [23].

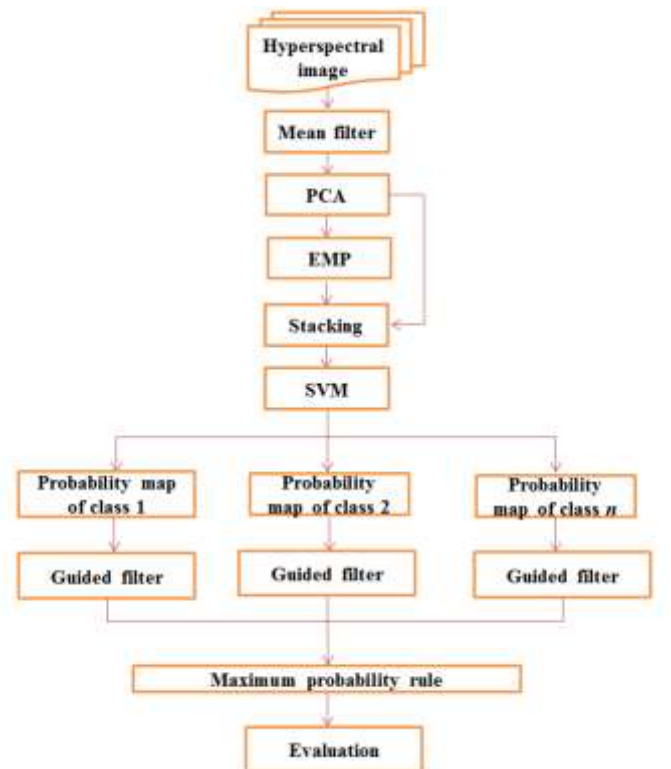Detailed information about EMP and GF are given in the next sub-sections.

Fig. 1. Block diagram of EMP-GF

a. *Morphological profiles*

Morphological opening and closing operators are based on elementary erosion and dilation operators as follows [30]:

Opening: $A \circ B = (A \ominus B) \oplus B$ (1)

Closing $\quad A \cdot B = (A \oplus B) \ominus B$ $\qquad$ (2)

In which A is the image, B is the structuring element (SE), $\ominus$ represents the erosion operator, and $\oplus$ is the dilation operator. Due to the modification of structures after applying the opening and closing transformations, [31,32] used morphological opening and closing by reconstruction for spatial feature extraction of the HSI. Opening γ_R and closing φ_R by reconstruction of image A are defined as:

$$\gamma_R^i = R_A^\delta(\varepsilon^i(A)) \qquad (3)$$

$$\varphi_R^i = R_A^\varepsilon(\delta^i(A)) \qquad (4)$$

Here, ε^i and δ^i are the erosion and dilation with the SE with the size i, and R_A^δ and R_A^ε are morphological dilation and erosion by reconstructions, respectively. Opening and closing by reconstructions are the connected operators which remove the structures that cannot contain the SE and totally preserve other structures. Commonly, different ranges of SE sizes are used for extracting the objects with different sizes. The morphological profile feature vector of each pixel in coordination of (*i, j*) which consists of the gray-level value of pixel (*Q*) and its values of opening and the closing by reconstruction with the different size of SE is defined as the following:

$$MP = \{\gamma_{R(i,j)}^i, \dots, Q_{(i,j)}, \dots, \varphi_{R(i,j)}^i\} \qquad (5)$$

In (1), φ_R^i is closing by reconstruction and γ_R^i is opening by reconstruction with SE of size *i*. Extended morphological profiles (EMP) can be defined by extending the concept of MP to multiband images. Based on the PCA transform of the original hyperspectral image, EMP is defined by (6):

$$EMP = \{MP^{PC1}, \dots, MP^{PCm}\} \qquad (6)$$

Where *m* is the number of desired PCs. In this study, EMP vector for each pixel stacked with PCA spectral features and formed the spatial-spectral vector.

b. *Guided filter*
Specifically, the classified image of SVM can be shown as the *n* number of binary classified maps, in which *n* is the number of classes. These binary maps commonly contain noisy classified pixels which degrade the classification accuracy. The post-processing stage based on the guided filter can eliminate these noisy classified pixels and therefore improve the classification accuracy.

In guided image filtering, q_i (smoothed probability map of SVM classifier for each class), is a linear transform of guidance image I (first PC or first three PCs) in a window ω_k centered at the pixel k [21]:

$$q_i = a_k I_i + b_k \quad, for \ i \in \omega_k \qquad (7)$$

Where a_k and b_k are some linear coefficients which are constant in ω_k. difference between q and filter input p (initial binary probability map of SVM for each class) is minimized:

$$E(a_k, b_k) = \sum_{i\in\omega_k}((a_k I_i + b_k - p_i)^2 + \epsilon\, a_k^2) \qquad (8)$$

Where ϵ is a regularization parameter. By solving the (8) these coefficients can be determined by (9) and (10):

$$a_k = \frac{\frac{1}{|\omega|}\sum_{i\in\omega_k}(I_i\, p_i - \mu_k \bar{p}_k)}{\sigma_k^2 + \epsilon} \qquad (9)$$

$$b_k = \bar{p}_k - a_k \mu_k \qquad (10)$$

Where μ_k and σ^2 are mean and variance of I in ω_k, $|\omega|$ is the number of pixels in ω_k, and $\bar{p}_k$ is the mean of p in ω_k. Guidance image can be gray or color images. After obtaining the smoothed classified maps of each class, the final label of each pixel is determined based on maximum probability rule as:

$$C = argmax_n \, P_{i,n} \qquad (11)$$

In which C is the final label of pixel i and $P_{i,n}$ is the probability map of pixel i in the class *n*.

3. Experimental Results
A. *Data sets*
Two real hyperspectral images are used in this study for studying the effectiveness of proposed EMP-GF. First one, Indian pines hyperspectral image, gathered by AVIRIS sensor from an agricultural area in Indiana of USA. It has 220 spectral bands that after discarding the noisy bands, 200 noise-free bands are used in the experiments. The distribution of 16 classes in this scene is shown in the ground truth map (GTM) of Fig. 2.a. The second data set, Pavia university hyperspectral image, was collected by ROSIS 3 sensor in 2003. This image has 115 spectral bands ranging from 0.43 to 0.86 μm. Dimensions of this image are 610×340 pixels and spatial resolution is 1.3m. Nine classes of urban land-cover are shown on its (GTM) of Fig. 2.b.
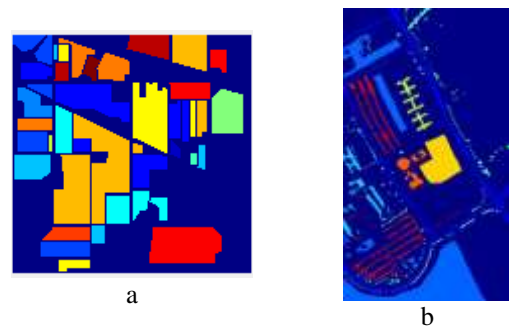

a

b

Fig. 2. Ground truth maps of a) Indian pines b) Pavia university

B. *Experiments setup*
EMPs are generated with disk shape SE with sizes of 3,5,7,9 and 11 from the first three PCs for both data sets. The dimensionality of HSIs is reduced via PCA and for Indian Pines first 69 features and for Pavia university first 15 features which contain 99% of information are considered as

final spectral features. The spatial-spectral feature vector is generated based on stacking the EMP and PCs. Resultant spatial-spectral vectors are classified via SVM classification. LIBSVM package is used for implementing the SVM classifier [33]. A polynomial kernel with degree 3 is used in SVM and features are mapped into [-255 to 255] [29]. Performance of classifier is evaluated based on four accuracy indices, overall accuracy(OA), kappa coefficient (kappa), average accuracy (AA) and average validity(AV) (for more information refer to [11]). Training samples are randomly chosen from approximately 5% labeled samples of GTM for Indian Pines and 1% of labeled samples of GMT for Pavia University and remaining labeled samples of GMTs are used as test samples. The first PC of the hyperspectral image is considered as gray guidance and the first three PCs are considered as color guidance images. Parameters of the guided filter (ϵ and window size) in all experiments are determined optimally by trial and error.

C. Ablation study and experimental results

This sub-section investigates the efficiency of each part of the proposed EPF-GF. Based on TABLE I and TABLE II, 6 different cases are considered as follows:

- PCA: In this case, classification is carried out with the only spectral PCs features.
- PCA+GFg: In this case, classification is carried out with the only spectral PCs features and a post-processing stage is done with guided filter and gray guidance image.
- PCA+GFc: In this case, classification is carried out with the only spectral PCs features and a post-processing stage is done with guided filter and color guidance image.
- PCA+EMP: In this case, classification is carried out with the stacked spatial-spectral (PCA+EMP) features.
- PCA+EMP+GFg: In this case, classification is carried out with the stacked spatial-spectral (PCA+EMP) features and a post-processing stage is done with guided filter and gray guidance image.
- PCA+EMP+GFc: In this case, classification is carried out with the stacked spatial-spectral (PCA+EMP) features and a post-processing stage is done with guided filter and color guidance image.

With attention to Fig. 3 and Fig. 4, it can be understood that many noisy classified pixels exist in PCA spectral-based classified maps. In column 3 (PCA+GFg) and 4 (PCA+GFc) of TABLE 1 and TABLE 2, gray and color guided filters are applied on probability maps of spectral-based classification, respectively. Based on rows 2 and 3 of Fig. 3 and Fig. 4, although the density of noisy classified pixels is hugely reduced, there are still some noisy labels in some regions. By using the spatial-spectral features (PCA+EMP, column 5 of TABLE I and TABLE II), the initially classified map is in some cases smoother than the case of PCA+GFc. By applying the gray and color guided filter on the probability maps of PCA+EMP the classification accuracies are even to the highest levels and the most homogeneous classified map is produced in case of PCA+EMP+GFc. Based on the experiments, generally, the color guided filter is superior in comparison to gray guided filter due to the better preservation of edges in the color guidance image [21].

Table. 1. Classification Results for Indian Pines

Accuracy	PCA	PCA+GFg	PCA+GFc	PCA+EMP	PCA+EMP+GFg	PCA+EMP+GFc
OA	82.94	93.37	91.92	88.99	96.28	96.82
Kappa	0.8	0.92	0.91	0.87	0.96	0.96
AA	85.45	95.17	90.04	88.49	95.41	97.23
AV	84.49	95.57	94.09	88.41	97.94	97.74

Table. 2. Classification Results for Pavia University

Accuracy	PCA	PCA+GFg	PCA+GFc	PCA+EMP	PCA+EMP+GFg	PCA+EMP+GFc
OA	93.99	97.31	95.75	98.83	99.06	99.43
Kappa	0.92	0.96	0.94	0.98	0.986	0.99
AA	93.10	96.53	95.28	98.56	98.74	99.3
AV	93.30	96.67	94.03	98.53	99.34	99.44

The final result of TABLE I and TABLE II in case of PCA+EMP+GFc demonstrated that proposed method with only 102 and 45 features for Indian Pines and Pavia University (with compression ratio about 2) reaches to the very high level of accuracy even when very few training samples (approximately 1%) are available. The fast and simple structure along with promising results of the proposed method increases the applicability of the proposed framework in different case studies of the HSI classification.
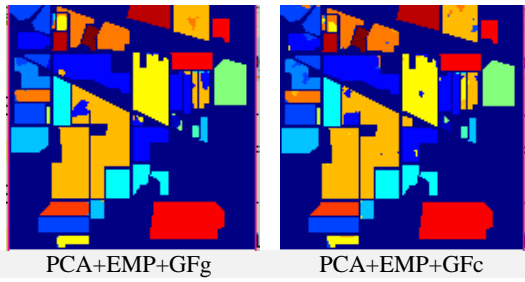

PCA　　　　　　　　PCA+EMP

PCA+GFg　　　　　　PCA+GFc

PCA+EMP+GFg   PCA+EMP+GFc
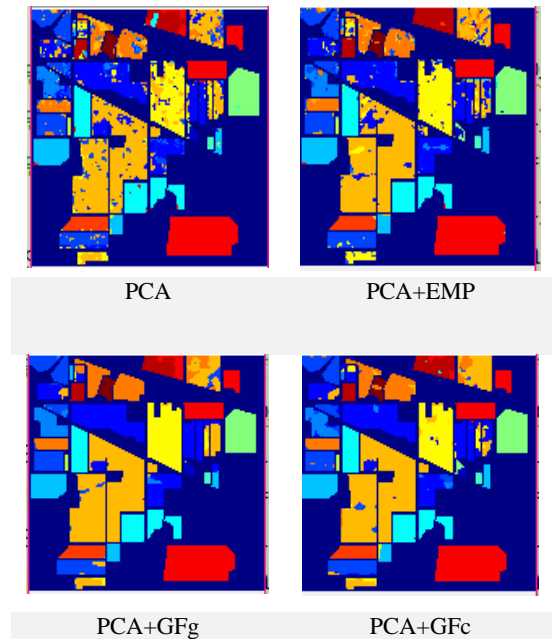
Fig. 3. Classified maps of Indian Pines

PCA   **PCA+EMP**

PCA+GFg   **PCA+GFc**

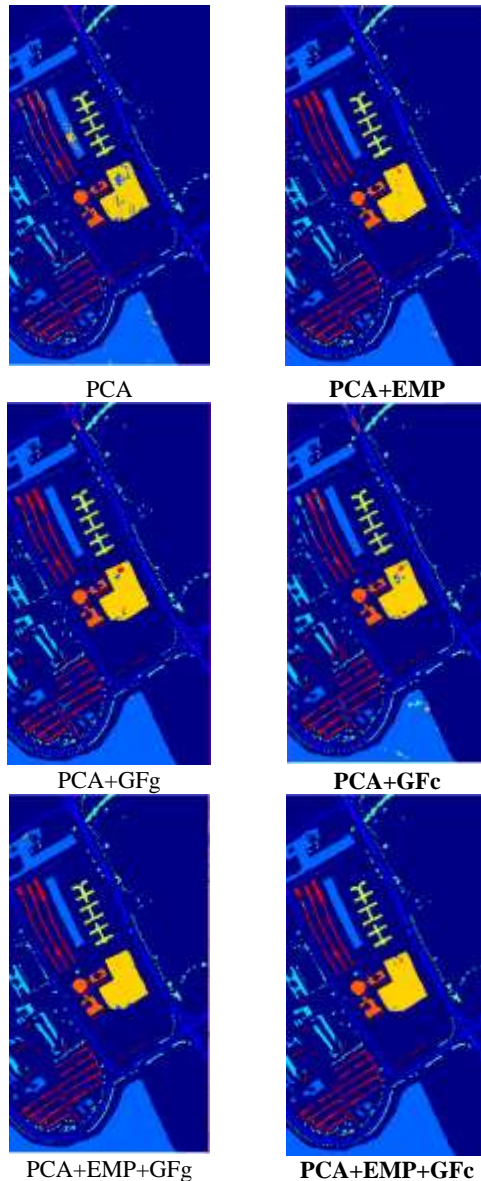PCA+EMP+GFg   **PCA+EMP+GFc**

Fig. 4. Classified maps of Pavia University

D. Comparison to recent methods

To evaluate the effectiveness of the proposed method, the classification accuracies of the proposed method have been compared with three state-of-the-art methods for the classification of hyperspectral images. Methods and their setups are as below:

- RPNET [27]: In this method, a deep model is simulated based on the PCA transform for extracting spatial-spectral features. Final extracted features are classified with SVM. Parameters of this method are tuned based on the original paper.

- JSaCR [26]: In the joint spatial-aware collaborative classification model (JSACR), both spatial and spectral features are used to induce the distance-weighted regularization terms. Also in this method, spatial information is added to representation objective function with a spatial regularization.

- R-HybridSN [28]: This method combines the 3D-2D-convolutional neural network (CNN), deep residual learning, and depth-separable convolutions for classification of hyperspectral images. The results of this method are presented based on the original paper.

Table. 3. Comparison with State-of-the-art Methods

	Indian Pines	Pavia University
Proposed method	**96.82**	**99.43**
RPNet (2018)	95.46	96.2
JSaCR (2017)	94.07	97.2
R-HybridSN (2019)	96.46	96.59

The obtained results of TABLE III proved the superiority of the proposed method over the RPNet, JSaCR, and R-HybridSN methods. It is worth noting that in addition to better classification accuracies, the proposed method has a very simpler framework than the other three competing methods.

4. Conclusion

A new spatial-spectral method is proposed in this paper for the classification of the HSI based on extended morphological profiles (EMP) and guided image filters. Based on this method, after the initial features extraction technique based on PCA, EMP is generated and stacked with spectral PCs. The resultant spatial-spectral feature vectors are classified by the SVM classifier. Guided filter with gray and color guidance images is applied on the probability map of each class and the final label of each pixel is determined based on maximum probability. Based on the final results, it is concluded that the proposed method based on the color guidance image has a simple structure and can reach a very high level of accuracy even when very few training samples are available. Combination of the multi-shape extended morphological profiles with a guided filter is suggested for future study.

References

[1] Z. A. Andekah, M. Naderan, and G. Akbarizade, "*Semi-supervised hyperspectral image classification using spatial-spectral features and superpixel-based sparse codes*". Presented at IEEE Iranian Conference on Electrical Engineering (ICEE). Tehran, Iran, (2017).

[2] Ch. Chang, "*Hyperspectral data processing: algorithm design and analysis*," John Wiley & Sons, (2013).

[3] M. Fauvel, J. Chanussot, and J. A. Benediktsson, "Kernel principal component analysis for the

classification of hyperspectral remote sensing data over urban areas," *EURASIP Journal on Advances in Signal Processing,* pp. 1-14, (2009).

[4] W. Li, S. Prasad, J. E. Fowler, L. M. Bruce, "Locality-preserving dimensionality reduction and classification for hyperspectral image analysis," *IEEE Transactions on Geoscience and Remote Sensing,* vol. 50, no. 4, pp. 1185-1198, (2011).

[5] Q. Wang, Z. Meng, and X. Li, "Locality adaptive discriminant analysis for spectral–spatial classification of hyperspectral images," *IEEE Geoscience and Remote Sensing Letters,* vol. 14, no. 11, pp. 2077-2081, (2017).

[6] Y. Dong, B. Du, L. Zhang, L. Zhang, "Dimensionality reduction and classification of hyperspectral images using ensemble discriminative local metric learning," *IEEE Transactions on Geoscience and Remote Sensing, vol. 55, no. 5,* pp. 2509-2524, (2017).

[7] .B. Guo, S. R. Gunn, R. I. Damper, J. D. Nelson., "Band selection for hyperspectral image classification using mutual information," *IEEE Geoscience and Remote Sensing Letters,* vol. 3, no. 4, pp. 522-526, (2006).

[8] J. Jiang, J. Ma, C. Chen, Z. Wang, Z. Cai, L.Wang. (2018). SuperPCA: A superpixelwise PCA approach for unsupervised feature extraction of hyperspectral imagery. *IEEE Transactions on Geoscience and Remote Sensing. 56(8)*, pp. 4581-4593.

[9] Beirami, Behnam Asghari, and Mehdi Mokhtarzade. (2020). Band Grouping SuperPCA for Feature Extraction and Extended Morphological Profile Production from Hyperspectral Images. *IEEE Geoscience and Remote Sensing Letters*. DOI: 10.1109/LGRS.2019.2958833

[10] L. Zhang, H. Su, and J. Shen, "Hyperspectral Dimensionality reduction based on multiscale superpixelwise kernel principal component analysis, *Remote Sensing*. vol. *11, no. 10*, pp. 1219.

[11]. B.A. Beirami and M. Mokhtarzade. (2017). SVM classification of hyperspectral images using the combination of spectral bands and Moran's I features. Presented at IEEE 10th Iranian Conference on Machine Vision and Image Processing (MVIP). Isfahan, Iran.

[12] Ayerdi, Borja, Ion Marqués, and Manuel Graña. "Spatially regularized semisupervised ensembles of extreme learning machines for hyperspectral image segmentation," *Neurocomputing,* vol. 149, pp. 373-386, (2015).

[13] Li, Wei, and Qian Du, "A survey on representation-based classification and detection in hyperspectral remote sensing imagery," *Pattern Recognition Letters,* vol. 83, pp. 115-123, (2016).

[14] F. Gao, Q. Wang, J. Dong, Q. Xu. "Spectral and spatial classification of hyperspectral images based on random multi-graphs," *Remote Sensing,* vol. 10, no. 8, pp. 1271, 2018. doi:10.3390/rs10081271.

[15] W. Zhao, X. Chen, J. Chen, Y. Qu, "Sample generation with self-attention generative adversarial Adaptation Network (SaGAAN) for Hyperspectral Image Classification," *Remote Sensing,* vol. 12, 5, pp. 843, (2020).

[16] A. Davari, H. C. Özkan, A. Maier, C. Riess, "Fast and efficient limited data hyperspectral remote sensing image classification via GMM-Based Synthetic Samples," *IEEE Journal of Selected Topics in Applied Earth Observations and Remote Sensing,* vol. 12, no. 7, pp. 2107-2120, (2019).

[17]. J. A. Benediktsson, J. A. Palmason, J. R. Sveinsson, "Classification of hyperspectral data from urban areas based on extended morphological profiles," *IEEE Transactions on Geoscience and Remote Sensing,* vol. 43, no. 3*,* pp. 480-491, (2005).

[18]. M. Pesaresi, and J. A. Benediktsson, "A new approach for the morphological segmentation of high-resolution satellite imagery," *IEEE transactions on Geoscience and Remote Sensing,* vol. 39, no. 2, pp. 309-320, (2001).

[19]. K. Tan, and P. Du. "Classification of hyperspectral image based on morphological profiles and multi-kernel SVM," Presented at IEEE 2nd Workshop on Hyperspectral Image and Signal Processing: Evolution in Remote Sensing (WHISPERS). Reykjavik, Iceland, (2010).

[20] B. Kumar, and O. Dikshit, "Hyperspectral image classification based on morphological profiles and decision fusion. *International Journal of Remote Sensing.* vol. 38, no. 20, pp. 5830-5854, (2017).

[21]. K. He, J. Sun, and X. Tang, "Guided image filtering. *IEEE transactions on Pattern Analysis and Machine Intelligence,* vol. 35, no. 6, pp. 1397-1409, (2001).

[22] H. Ma, W. Feng, X. Cao, L. Wang "Classification of hyperspectral data based on guided filtering and random forest," in *Proc.* ISPRS-International Archives of the Photogrammetry, Remote Sensing and Spatial Information Sciences, 2017, pp. 821-824.

[23]. Kang, X., S. Li, and J.A. Benediktsson (2014). Spectral–spatial hyperspectral image classification with edge-preserving filtering. *IEEE Transactions on Geoscience and Remote Sensing. 52(5),* pp. 2666-2677.

[24] B. Pan, Z. Shi, and X. Xu. "Hierarchical guidance filtering-based ensemble classification for hyperspectral images," *IEEE Transactions on Geoscience and Remote Sensing,* vol. 55, no. 7, pp. 4177-4189, (2019).

[25]. X. Cao, B. Ji, Y. Ji, L. Wang, L. Jiao, "Hyperspectral image classification based on filtering: a comparative study,". *Journal of Applied Remote Sensing,* vol. 11, no. 3, pp. 035007-1 -035007-19, 2017. doi: 10.1117/1. JRS.11.035007.

[26] J. Jiang, C. Chen, Y. Yu, X. Jiang, J. Ma, "Spatial-aware collaborative representation for hyperspectral remote sensing image classification," I*EEE Geoscience and Remote Sensing Letters,* vol. 14, no. 3, pp. 404-408, (2017).

[27] Y. Xu, B. Du, F. Zhang, L. Zhang, "Hyperspectral image classification via a random patches network," *ISPRS Journal of Photogrammetry and Remote Sensing,* vol. 142, pp. 344-357, (2018).

[28] F. Feng, S. Wang, C. Wang, J. Zhang, "Learning deep hierarchical spatial–spectral features for hyperspectral image classification based on residual 3D-2D CNN. *Sensors,* vol. 19, no. 23, pp. 5276, (2019).

[29] F. Mirzapour, and H. Ghassemian. "Moment-based feature extraction from high spatial resolution

hyperspectral images," *International Journal of Remote Sensing,* vol. 37, no. 6, pp. 1349-1361, (2016.

[30]. R.C. Gonzalez, "Digital image processing," Prentice hall, (2016).

[31]. M. Fauvel, J. A. Benediktsson, J. Chanussot, J. R. Sveinsson, "Spectral and spatial classification of hyperspectral data using SVMs and morphological profiles," *IEEE Transactions on Geoscience and Remote Sensing*, vol. 46, no. 11, pp. 3804-3814, (2008).

[32] P. Soille, "Morphological image analysis: principles and applications," *Springer Science & Business Media*, (2013).

[33]. C. C. Chang, and C. J. Lin, "LIBSVM: a library for support vector machines," *ACM Transactions on Intelligent Systems and Technology*, vol. 2, no. 3, pp. 27:1-27:27, (2011).